THERMAL CHARACTERIZATION OF SEMICONDUCTOR BI_2TE_3 MATERIALS USING DSC

RADU SETNESCU[1,2], IULIAN BANCUTA[1], TANTA SETNESCU[1,2], VALERICA CIMPOCA[1], SILVIU JIPA[1,2], ION V. POPESCU[1]

[1]*Valahia University of Targoviste, Faculty of Science and Arts, 130082, Targoviste, Romania*

[2] *National Institute for R&D in Electrical Engineering (ICPE-CA), 030138, Bucharest, Romania*

Abstract: *The behavior upon heating (30 – 650 ^{o} C) and subsequent cooling (to room temperature) has been studied for both n and p type semiconductors based on Bi_2Te_3 alloys. The elemental composition of the studied alloys has been established by EDXRF analysis. The materials are used in manufacture of thermoelectric generators and coolers.*

Keywords: *semiconductor, DSC, EDXRF*

1. INTRODUCTION

Bismuth telluride (Bi_2Te_3) presents gray, hexagonal platelets with a melting point of 585 °C and a density of 7.7 g/cm^3 [1]. It is a narrow gap layered semiconductor with a trigonal unit cell and with large Seebeck coefficients and, as such, it has been used in thermoelectric refrigeration power generation applications for a long time [2]. The structure of both the valence and conduction bands can be described by a *six-valley ellipsoid* model [1]. Bi_2Te_3 cleaves easily along the trigonal axis due to van der Waals bonding of the neighboring tellurium atoms. To avoid these phenomena that strongly affect the mechanical properties, Bi_2Te_3 based materials must be polycrystalline [1]. The use of Sb and Se alloys inside of pure Bi_2Se_3 is requested because the Seebeck coefficient of Bi_2Te_3 becomes compensated around the room temperature [1, 3].

Recently, it was attempted to improve the efficiency of the Bi_2Te_3 based thermoelectric materials through nano-structures such as nano-wires or thin films [4]. Such a material presented an improved Seebeck coefficient (i.e. (-287 μV/K la 54 K). However, it shall be noted that the high values of Seebeck coefficient will result in a decrease of charge carriers and, hence, in a decrease of the electrical conductivity [5].

In paper [6], it was reported a material based on Bi_2Te_3 presenting high electrical conductivity ($1.1 \cdot 10^5$ S·m/m^2) and a very low thermal conductivity (1.20 W·m/m^2·K), similar to that of the ordinary glass. These kind of thermoelectric materials are very interesting as PGEC-like (phonon glass and electron crystal) materials [7]. Generally, the most efficient Bi_2Te_3 – Bi_2Se_3 thermoelectric materials, of n-type, are those containing less than 33.3 % (mol/mol) Bi_2Se_3 [8, 9].

Thermal analysis methods are able to provide useful information concerning the structural characteristic and thermal behavior of the materials. In the case of the thermoelectric materials, Differential Scanning Calorimetry (DSC) can be used for the analysis of phase transitions or the specific heat, melting/crystallization behavior, solid-solid transitions, polymorphism, degree of crystallinity, oxidative stability, purity determinations or the thermokinetics of various processes; the thermal stability yields information on the maximum service temperature. TG (Thermogravimetric analysis) is useful for quantitative weight-characterization of the mass changes, decomposition, decomposition or corrosion.

Other thermal analysis methods and instruments, such as DMA (Dynamic Mechanical Analysis) LFA (Laser Flash Analysis) – are suitable to measure the thermal expansion and respectively the Thermal Conductivity on Small and Thin Samples.

The application of the thermal analysis methods in characterization of Bi-Te materials is reported in several papers as for example [9-11]. The structure of phase diagram of the system (Bi_2Te_3)-(BiI_3) and the structure of the resulted BiTeI crystal are described in paper [12] and the critical concentration for tellurium precipitation is reported in paper [13].

In paper [9], the thermal analysis has been performed by a pyrometer (NTR 72 type) and a Pt-Pt/Rh thermocouple. The heating (up to 900 ^{o}C) and the cooling were carried out in Stepanov quartz bulbs evacuated at 0.1 Pa and using anhydrous alumina as reference material. The *solidus* points were identified of the heating curve and the *liquidus* ones were identified on the cooling curve.

In the present work, the compositional (by EDXRF) and the thermal and thermal-oxidative (by DSC) characterization of two different Bi-Te based alloys was attempted in order to highlight the differences between the studied materials.

2. EXPERIMENTAL

Two Bi-Te based semiconductor materials were studied: one is of type p and will be named below as 6p material; the other one, named the *material 7n*, is of n type. Both materials were synthesized at the National R&D Institute for Electrochemistry and Condensed Matter in Timisoara, Romania. The chemical composition of the studied materials has been established by EDXRF (*Energy Dispersive X-Ray Fluorescence*) spectrometry analysis using a spectrometer Elva X Light (Elvatech Ltd., Kiev, Ukraine). Each material sample has been exposed to X-ray irradiation for 300 s. The X-ray fluorescence spectra were off-line processed by Elva X specific software.

The DSC (*Differential Scanning Calorimetry*) was performed by a Setram 131 evo instrument (Setaram Instrumentation, Caluire, France) in either inert (nitrogen) or oxidant (air) atmosphere at a constant heating rate. The gas (nitrogen or air) flow rate was 50 mL/min., and the temperature range was 25 – 650 ^{o}C (for the measurements in nitrogen atmosphere) or 25 – 450 ^{o}C (for the measurements in air atmosphere). The weight of the DSC samples was 12 – 15 mg, powdered material. The DSC measurements were performed in either alumina (for the measurements in nitrogen, up to 650 ^{o}C) or aluminium crucibles (for the measurements in air, up to 450 ^{o}C). The oxidation induction temperature has been determined according to reference standards [14, 15] as the temperature corresponding to the oxidation process onset.

3. RESULTS AND DISCUSSION

3.1. EDXRF DATA ON ELEMENTAL ANALYSIS

The empirical formulas, presented below, of the studied materials were calculated using the results of the elemental analysis summarized in Table 1. In this form, the compositional data enable to make a clearer difference between the studied materials:

- material 6p: $Bi_{116}Te_{6.36}Se_{1.28}Cu$
- material 7n: $Bi_{22}Te_{6.85}Se_{6.92}Fe_{1.27}Ni_{1.88}Zn$

If we assume that Bi and Te are combined as Bi_2Te_3 and Bi and Se are combined as Bi_2Se_3, the following conclusions can be drawn:

- both materials, but especially the material 6p, have an important content of apparently free bismuth (non combined as Bi_2Te_3, Bi_2Se_3);
- the molar ratio Bi_2Te_3/Bi_2Se_3 is around 5:1 for the material 6p and around 1:1 for the material 7n;
- the Bi excess is considerably higher for the material 6p.

Table 1. Elemental composition of the studied materials as found by EDXRF

Material		Elemental composition of the material (%)						
		Se	Cu	Fe	Ni	Te	Bi	Zn
6p	% (m/m)	0.4	0.24	0	0	3.2	96.6	
	mol	0.0051	0.0038	0	0	0.0251	0.4601	-
	% (mol/mol)	1.02	0.8	0	0	5.08	93.1	-
7n	% (m/m)	9.02	0	1.2	1.8	14.5	72.4	1.08
	mol	0.114	0	0.021	0.031	0.113	0.364	0.0165
	% (mol/mol)	17.28	0	3.18	4.70	17.14	55.2	2.50

3.2. DSC MEASUREMENTS IN INERT ATMOSPHERE

Occasionally, the DSC curves of the materials presented upon heating an endothermic peak at around 265 ^{o} C, which is close to the melting point of bismuth, hence it can be assigned to free bismuth melting (Figs. 1 and 2). As the area of this peak, i.e. the variation of enthalpy related to this process, is very small, it can be concluded that only few amount of free Bi is present in the material 7n.

The peak at 265 ^{o} C was no observed in the material 6p, even a high Bi content was observed in the elemental analysis. This behavior can be explained by the possible occurrence of some solid solutions which can stabilize the important excess of Bi [9].

For the endothermic peak regularly observed at ca. 230 ^{o} C in both materials (Table 2 and Figs. 1 and 2), there is no a clear assignment. It is probably due to a structural transition and could be related to loss of the thermoelectric properties at elevated temperature. The process is reversible, upon the cooling, this peak is again observed, but as an endothermic peak.

Table 2. DSC parameters of the peaks at ~ 230 ^{o}C si ~265 ^{o}C for the materials 6p and 7n

Material	Heating				Cooling			
	Peak I		Peak II		Peak I		Peak II	
	T_m (^{o}C)	ΔH (J/g)	T_m (^{o}C)	ΔH (J/g)	T_m (^{o}C)	ΔH (J/g)	T_m (^{o}C)	ΔH (J/g)
6p	232*	0.742	no peak		210	-0.841	no peak	
	224*	0.732	no peak		199	-0.915	no peak	
	233*	1.085	no peak		186	-1.038	no peak	
	233**	1.146	no peak		190	-1.233	no peak	
7n***	230	0.463	267	0.345	174	-0.617	no peak	
	230	0.516	no peak		212	-0.702	262	-0.23
	231	0.492	264	0.213	184	-0.897	262	-0.35

*Successive scanning of a same sample

**Air atmosphere

***The three series of data for 7n material were obtained by repeated scanning of a same sample; between the first and the second scanning, there are 100 h; the second and the third ones were successive

For the material 7n, the peak at ~230 ^{o} C appeared each time, even at repeated heating-cooling cycles. The thermal effect when cooling appears to be systematically higher than that observed upon heating, and the peak temperatures are lower than those observed upon heating. The latter effect appears similar to crystallization while the former could be related to the thermoelectric properties of this material.

The material 6n presented only the peak at ~230 ^{o} C, except the first scanning in a case (possibly material heterogeneity).

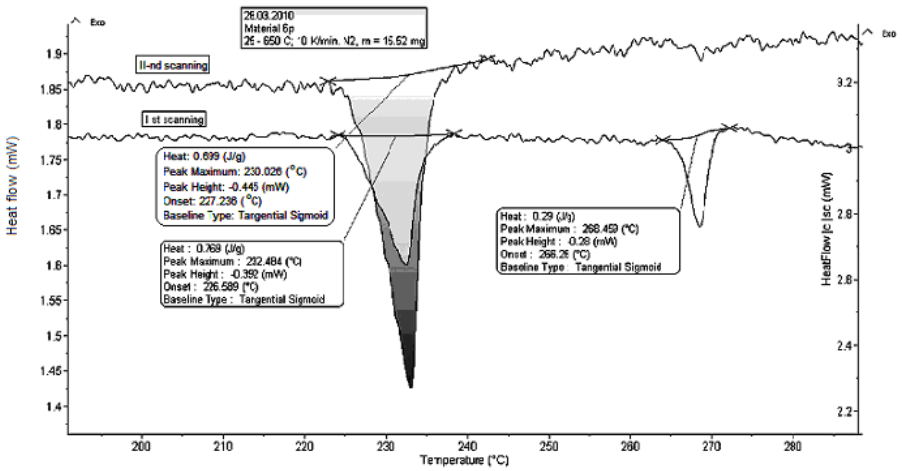

Fig. 1. DSC curves of the material 6p: the peaks at ~ 230 °C and ~ 265 °C (successive scanning of a same sample). Measurement conditions: heating rate: 10 K/min. T = 25 – 650 °C, nitrogen atmosphere

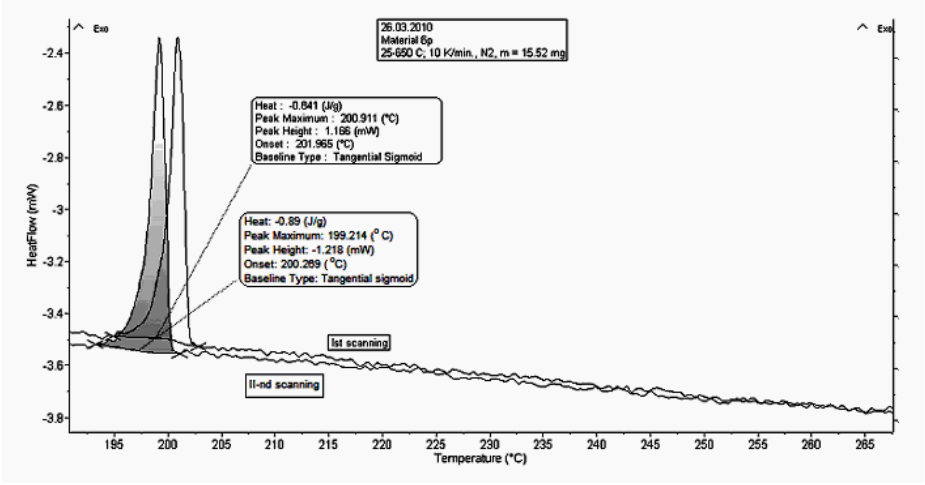

Fig. 2. DSC curves of the material 6p: the peak at ~ 230 °C (successive scanning of a same sample). Measurement conditions: cooling rate: 10 K/min. T = 650 – 25 °C; nitrogen atmosphere

For both materials, the DSC heating curves in the melting region are simpler than the cooling ones in the crystallization region (Figs. 4 and 5). The melting temperatures of both materials are considerably higher than the melting point of the pure bismuth, indicating that almost the bismuth is in a stable form, metallic combination or solution. The melting temperatures of the studied materials are close to the melting point of pure Bi_2Te_3 (585 °C), but higher than this value.

Upon the first scanning, in the melting region of the material 6p, only one peak, corresponding the single melting processes was observed (Table 3). It is due probably to the melting of a solution with high bismuth concentration. When the same sample is re-scanned in the same conditions, a second peak appears at ~ 547 °C, with a shoulder at 535 °C suggesting the formation of a new combination.

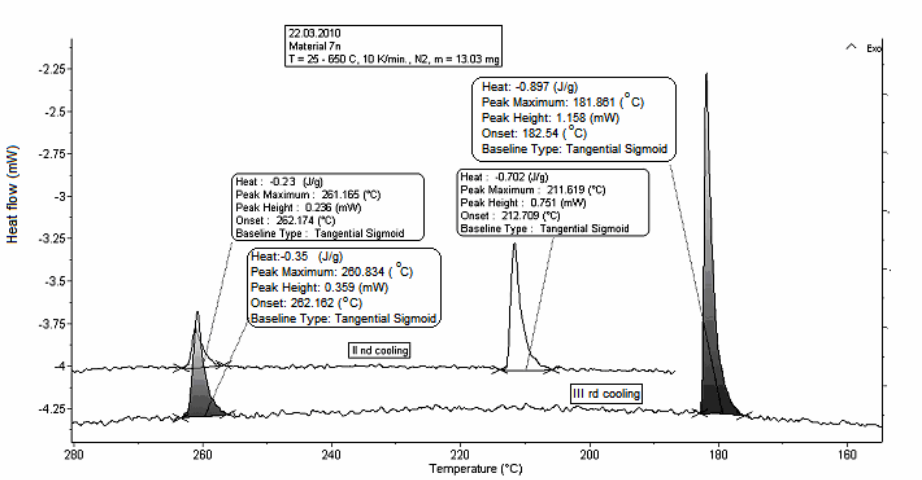

Fig. 3. DSC curves of the material 7n: the peaks at ~ 230 °C and ~ 265 °C (successive scanning of a same sample). Measurement conditions: cooling rate: 10 K/min. T = 650 – 25 °C; nitrogen atmosphere

It was observed also that the material 6p is quite volatile at high temperatures: the volatilization of small amounts of metal, probably bismuth was observed.

Upon the crystallization of the material 6p, it was observed an exothermic effect with 2 main peaks (Fig. 5) at 597 °C and 594 °C and a series of shoulders in the range 580 – 594 °C, indicating the separation form the solution of several combinations with different structure and composition. As upon a new scanning of the same sample, the structure of the melting region is simpler (see above), it can be concluded that the species responsible for the crystallization region exist in the liquid state only.

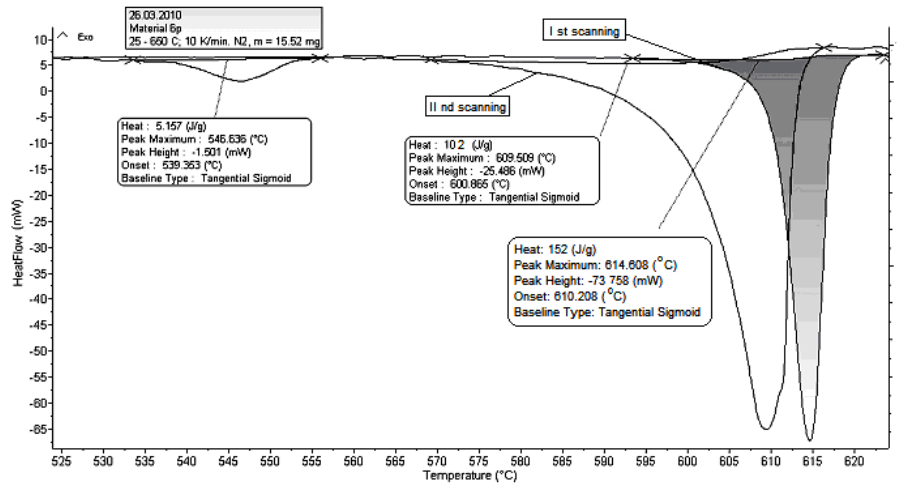

Fig. 4. DSC curves of the material 6p (successive scanning of a same sample); focus on the melting region. Measurement conditions: heating rate: 10 K/min. T = 25 – 650 °C; nitrogen atmosphere

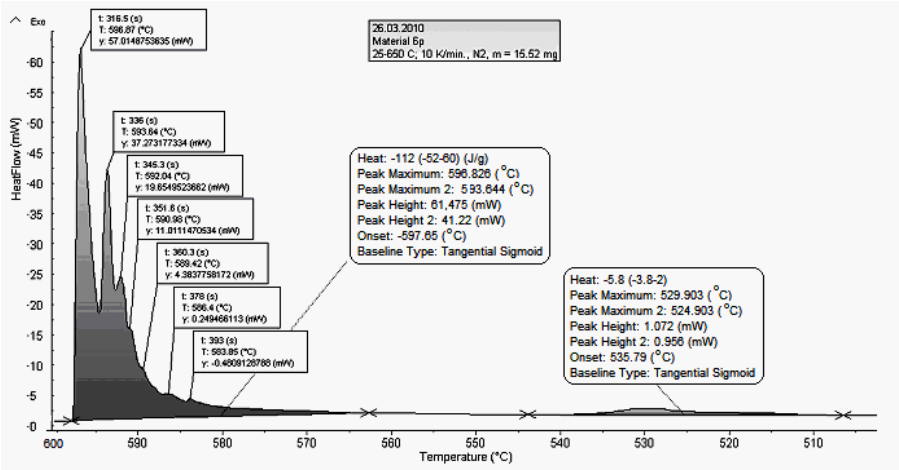

Fig. 5. DSC curve of the material 6p crystallization. Measurement conditions: cooling rate: 10 K/min. T = 650 – 25 °C; nitrogen atmosphere

When heating the sample 7n, the melting behavior is similar to that of the sample 6p (Table 3, Fig. 6), but the material is practically non-volatile in the studied temperature range (25 – 650 °C), The main peak is at ~600 °C; a smaller but wider peak is observed 578 °C. On a second scan of a same sample, a left-shifting of both peaks is observed (to 594 °C and 562 °C respectively); the second peak became greater and sharper.

The crystallization DSC curve of the material 7n is different to that of the material 6p: it presents two main regions: one presents two peaks, at 584 °C and 582°C and several other shoulders (Table 3) is the main melting process. The other one is the isolated low temperature peak, which is observed at 549 °C.

The differences in parameters of DSC crystallization curves between the materials 6p and 7n indicate the occurrence of different compounds in the liquid state. The nature of these compounds remains to be clarified, but it can be said that DSC enable to observe the differences between the thermoelectric materials and to characterize their thermal behavior.

DSC MEASUREMENTS IN AIR ATMOSPHERE

Heated in the presence of air, up to 450 °C, both materials presented the same DSC peak at ~230 °C observed in nitrogen. A steady increase of the heat flow as the temperature increased. This increase, without a peak, can however suggest an exothermic process, like oxidation. The induction temperatures (OOT) of these processes were estimated to be 270 °C for the material 7n and 268 °C for the material 6p. The latter material presented also a well resolved exothermic peak with OOT' = 277 °C (see Fig. 7), which can be also assigned to an oxidation process. As the visual examination of the powders after the DSC measurement in air shown that the sample 6p changed significantly its appearance (it became black mat) while the sample 7n kept its initial metallic brightness, this small peak can be related to oxidation. Therefore, it can be concluded that a clear oxidation process occurs in the material 6p with onset at 277 °C; no similar oxidation process is observed the case of the material 7n.

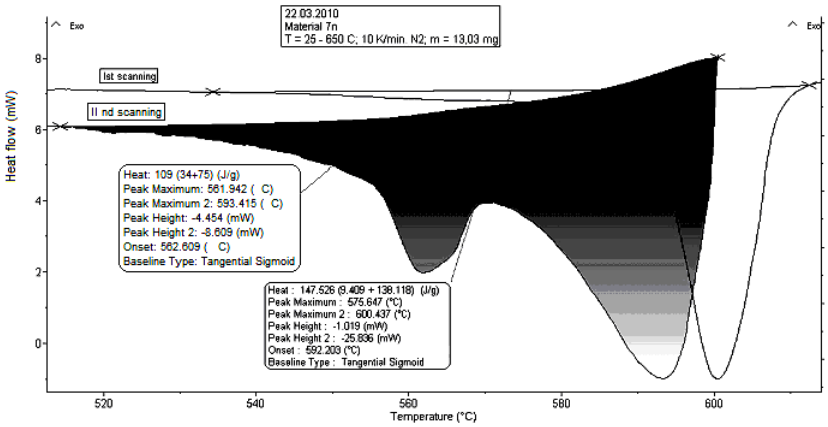

Fig. 6. DSC curves of the material 7n (successive scanning of a same sample); focus on the melting region. Measurement conditions: heating rate: 10 K/min. T = 25 – 650 ^{o}C; nitrogen atmosphere

Table 3. DSC parameters of the melting and crystallization for the materials 6p and 7n

Material	Melting				Crystallization						
	Peak I (main)		Peak II (secondary)		Peak I (high temperature)		Peak II (low temperature)		Other peaks (T_m, ^{o}C)	Peak III	
	T_m (^{o}C)	ΔH (J/g)	T_m (^{o}C)	ΔH (J/g)	T_m (^{o}C)	ΔH (J/g)	T_m (^{o}C)	ΔH (J/g)		T_m (^{o}C)	ΔH (J/g)
6p - Ist scanning	615	152	-	-	597	-52	594	-60	592, 591, 589, 586, 584	529	-5.8
6p – IInd scanning	609	102	547	5.2	595	-56	589	-29	591, 587, 583, 581, 580, 575	529	-9.5
7n – Ist scanning	600	138	576	9.4	591	-C70	549	-49	593, 549, 537, 522, 513, 506, 500	-	-
7n – IInd scanning	593	75	562	34	584	-45	550	-54	549, 540, 524	-	-

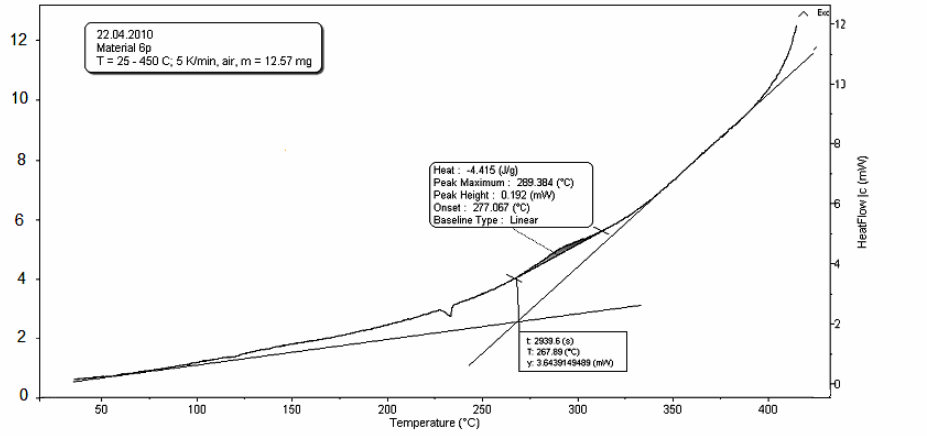

Fig. 7. DSC curves of the material 6p – heating in air atmosphere: 5 K/min. T = 25 – 450 ^{o}C; air atmosphere

4. CONCLUSIONS

The DSC study of the Bi-Te based materials indicated that few amount of Bi is in free, uncombined state. It tends to completely disappear after heating at elevated temperatures (such as 450 ^{o}C in air or 650 ^{o}C in nitrogen atmosphere), especially in the case of 6p material.

Differences between the melting curves as well as between the crystallization curves were observed, indicating a different nature of the intermetallic compounds in the studied materials.

For both materials, the crystallization curves were more complex than the melting ones. The material 6p present an exothermic, possibly oxidation process, which starts at ~280 ^{o}C. No similar process occurs in the material 7n, that appears more stable to oxidation.

Generally, the material 7n appears more stable form the point of view of thermal behavior than 6p.

REFERENCES

[1] Caywood, L. P. *Phys. Rev. B.*, **2**, 3209, 1970.
[2] Notingher P., Ifrim A., "Materiale Electrotehnice", Ed. Didactica si Pedagogica, Bucuresti, 1992.
[3] Satterthwaite, C. B., *Phys. Rev.* **108**, 1164, 1957.
[4] Tan, J., Thermoelectric properties of bismuth telluride thin films deposited by radio frequency magnetron sputtering, *Proceedings of the SPIE*, **5836**, 711, 2005.
[5] Goldsmid, H.J., Sheard, A.R. and Wright, D.A. *Br. J. Appl. Phys.* **9**, 365, 1958.
[6] Takiishi, M. et all, *Thermophys Prop*, **27**, 24-26, 2006.
[7] Slack, G. A. et al. *J. Appl. Phys*., **76**, 1665-1671, 1994.
[8] Goltsmann, B.M., Kudinov, V.A., Smirnov, I.A., *Bi_2Te_3-based semiconductors thermoelectric materials*, M. Nauka Publishing House, Moscow 1972, cited in ref. [8]
[9] Sokolov, O.B., Skipidarov, S.Ya., Duvankov, N.I., Shabunina, G.G., *J. Crystal Growth*, **262**, 442 – 448, 2004.
[10] Ji X.H., Zhao X.B., Zhang Y.H., Sun T., Ni H.L., Lu B.H., Novel thermoelectric Bi_2Te_3 nanotubes and nanocapsules prepared by hydrothermal synthesis, *Proceedings of the 23rd International Conference on Thermoelectrics, ICT2004*, Australia, 2004. http://zts.cvining.com/system/files/Ji-ICT-2004.pdf
[11] Kim, S.W., Kimura Y., Mishima Y., *Science and Technology of Advanced Materials*, **5**, 485–489, 2004.
[12] Tomokiyo, A, Okada, T. and Kawano, S., *Jpn. J. Appl. Phys*., **16**, 291-298, 1977.
[13] Hasezaki, K., Hamachiyo, T., Ashida, M., Ueda, T., and Noda, Y., *Materials Transactions*, **51**(05), 863-867, 2010.
[14] *ASTM-E-2009-02: Standard Test Method for Oxidation Onset Temperature of Hydrocarbons by Differential Scanning Calorimetry*
[15] ISO 11357-6: 2008 *Plastics - Differential Scanning Calorimetry (DSC) - Part 6: Determination of oxidation induction time (isothermal OIT) and oxidation induction temperature (dynamic OIT)*

Manuscript received: 28.04.2010
Accepted paper: 30.05.2010
Published online: 22.06.2010